Molecular Vision 2006; 12:892-901 <http://www.molvis.org/molvis/v12/a101/>
Received 22 February 2006 | Accepted 4 August 2006 | Published 10 August 2006

Retinoschisin forms a multimolecular complex with extracellular matrix and cytoplasmic proteins: interactions with β2 laminin and αB-crystallin

Marie-France Steiner-Champliaud,[1] José Sahel,[1] David Hicks[1,2]

[1]Laboratoire de Physiopathologie Cellulaire et Moléculaire de la Rétine, INSERM U 592, Hópital St. Antoine, Paris, France; [2]Laboratoire de Neurobiologie des Rythmes, CNRS UMR 7168/LC2, Strasbourg, France

Purpose: X-linked juvenile retinoschisis is a rare early-onset retinal degeneration characterized by the formation of cysts and loss of the electroretinogram "b" wave. The affected gene normally codes for retinoschisin (Rs1), a secreted protein containing a large discoidin homology domain. Rs1 seems to be principally synthesized in the photoreceptors, but its structure and spectrum of effects when mutated indicates association with other proteins. The present study searched for retinal proteins capable of interacting with Rs1.

Methods: Western blotting and RT-PCR of isolated outer nuclear (photoreceptors), inner nuclear and ganglion cell layers, and cell culture compartments were performed to verify sites of Rs1 synthesis and distribution. Potential Rs1 binding partners were searched for with affinity columns generated using specific Rs1- and β2 laminin-antisera. Following loading with total protein extracts from porcine retina, bound proteins were acid eluted and visualized by Coomassie blue staining of SDS-polyacrylamide gels, and selected bands were excised for tryptic peptide digestion and sequencing. Using single and double labeled immunohistochemistry, candidate binding partner distributions with that of Rs1.

Results: Whereas Rs1 mRNA was confined to the outer nuclear layer, Rs1 protein was found throughout the retina, including within the ganglion cell layer. One protein that was retained on Rs1 affinity columns was identified as αB crystallin, which showed partially overlapping distribution with Rs1 in the retina, mainly in the interphotoreceptor matrix and outer plexiform layer. Also, β2 laminin columns retained Rs1, and again shared partial distribution patterns. Finally, unidentified peanut agglutinin-binding proteins from the retina also bound to Rs1, αB crystallin and β2 laminin.

Conclusions: Taken together, these data demonstrate that Rs1 associates with different proteins during its synthesis and secretion, forming a multimolecular complex which presumably forms a stabilizing scaffold for retinal synapses, and possibly overall tissue integrity.

X-linked juvenile retinoschisis is a recessively inherited, bilateral retinal degeneration affecting young males [1-4]. Affected individuals typically experience mild to severe loss in visual acuity in the first decade of life followed by progressive atrophy of the macula in mid to later years. About 50% of the patients also suffer from a decrease in visual field. Electroretinograms (ERGs) of most affected individuals exhibit normal a-waves, characteristic of normal photoreceptor function, but severely reduced b-waves, indicating a perturbation in synaptic transmission between photoreceptors and second order neurones (bipolar and horizontal cells) [5-7].

The gene (*xlrs1*) affected in X-linked juvenile retinoschisis has been identified by positional cloning [8], and consists of six exons encoding a 224 amino acid protein containing a 23 amino acid hydrophobic leader sequence with a consensus signal peptidase cleavage site. Retinoschisin protein (Rs1) consists mostly of a discoidin-like domain that is found in a heterogeneous family of proteins implicated in cell adhesion [9-11]. A recent studies [12] demonstrated it forms multimers through disulfide bonding. A spectrum of genetic mutations is found in individuals with X-linked retinoschisis, including missense and nonsense mutations, insertion and deletion mutations, intragenic deletions, and splice-site mutations [4,13,14]. These mutations occur chiefly within the discoidin-like domain, and result in protein misfolding, failure to insert into the retinoplasmic membrane and defective formation of multimers. Several studies indicate that missorting, protein retention and compromised subunit oligomerization as a consequence of *xlrs1* mutations, are major pathogenic mechanisms [15-17]. In situ hybridization studies have shown that *xlrs1* mRNA is uniquely expressed in photoreceptors [18-20]. Recent studies by the same group indicate that the protein is recaptured from the interphotoreceptor matrix by pinocytosis at the level of the apical microvillosities of the Müller glia, then transported downward into the interior of the tissue and subsequently re-released near its target sites [21]. Other groups have contested this model, and report in addition to expression in photoreceptors, protein localization in the inner nuclear and ganglion cell layers [22,23], consistent with the observed clinical manifestations of retinal splitting [4].

xlrs1 null mice display a retinal phenotype similar to that observed in humans, namely frequent cystoid spaces and splitting of inner retinal layers, together with a marked reduction in ERG b-wave amplitude [24]. Ultrastructural observation of

Correspondence to: Dr. David Hicks, Laboratoire de Neurobiologie des Rythmes, CNRS UMR 7168/LC2, INCI, 5, rue Blaise Pascal, 67084 Strasbourg Cedex, France; Phone: 33 388 45 67 23; FAX: 33 388 45 66 54; email: photoreceptor67@hotmail.com

these mice demonstrated structural abnormalities of synapses within the outer plexiform layer, including disorganized ribbons and large extracellular spaces. Viral-mediated gene therapy of *xlrs1* null mice is able to rescue and even reverse the degenerative effects [25,26]. Since Rs1 is a secreted protein, its effects on synaptic organization would imply interaction with other molecules, both resident in the extracellular matrix (ECM) and within cells. We have generated affinity columns using anti-Rs1 polyclonal antibody, as well as candidate retinal ECM proteins, to examine potential molecular interactions. Both β2 laminin and αB crystallin emerge as candidate binding partners, as well as unidentified glycoproteins. In addition, separation of retinal layers by vibratome sectioning revealed *xlrs1* mRNA only in the photoreceptor layer, while Rs1 protein was detected in abundance throughout the retina, including the ganglion cell layer.

METHODS

Antibodies: Rabbit polyclonal anti-Rs1 antiserum was raised against the oligopeptide LSTEDEGEDPWYQKA (amino acid residues 23-37) conjugated to keyhole limpet hemocyanin and affinity purified on a HitrapTM Protein G HP (Amersham Pharmacia Biotech AB, Uppsala, Sweden). Antibody specificity was verified by western blotting and immunohistochemistry. The D5 monoclonal antibody against laminin β2 chain was a generous gift of Dr. W. Brunken (Tufts University, Boston, MA) [27]. The anti-αB-crystallin monoclonal antibody was purchased from Stressgen Biotechnology (Victoria, BC, Canada). Biotinylated Peanut Agglutinin (PNA) was purchased

Table 1. Primers

mRNA	Primer sequence (5'-3')	Product size (bp)
Rs1	F: TCATCGACAGAGGATGAGGGTGAG	507
	R: CCTGAGTAAGTTCTGAACTGTAGA	
mGluR6	F: CCAGTCAGATGATTCCACCCGG	335
	R: ATTGGCCCACGGCCTGGTAC	
Rhodopsin	F: ATTCACCACCACCCTCTACACC	514
	R: ATAGTAGTACCAGTAGAAGAAG	

Forward and reverse primers were used for RT-PCR analyses.

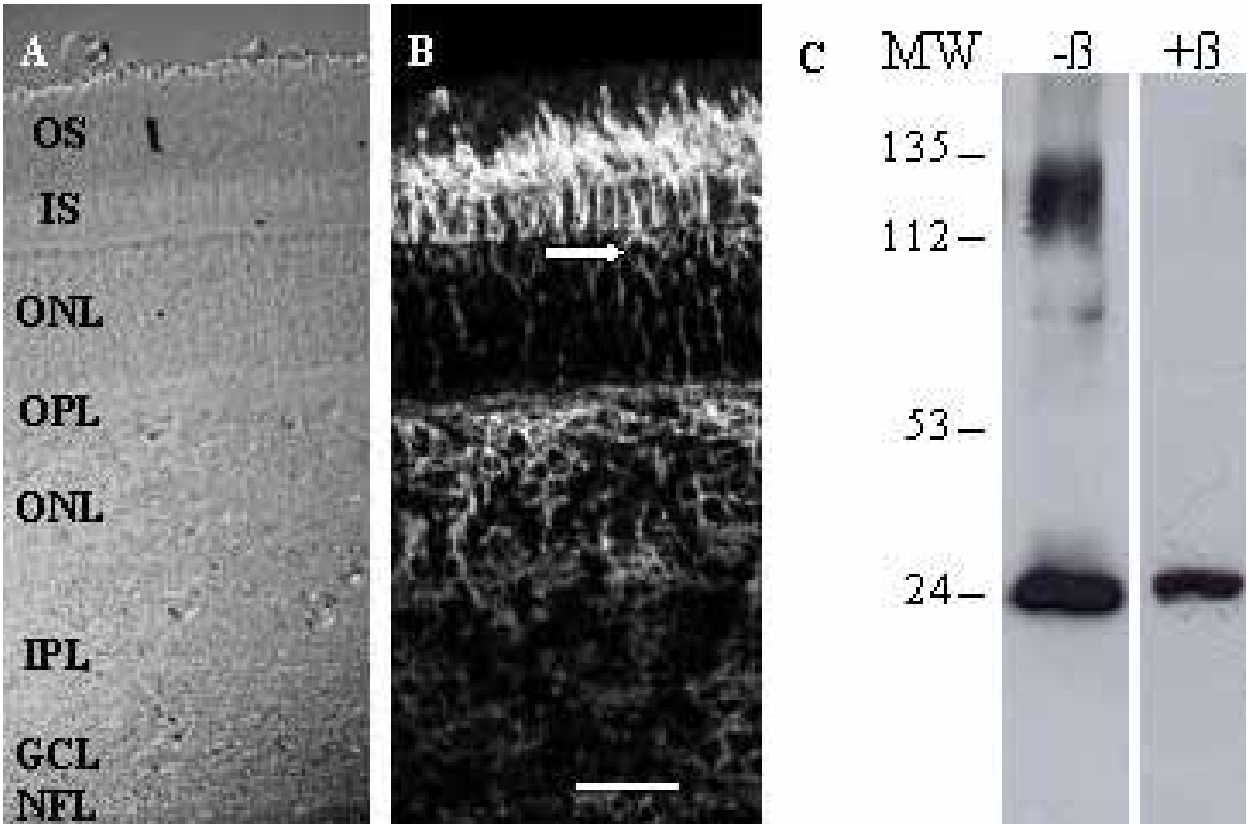

Figure 1. Rs1 Immunostaining and western blotting in adult pig retina. When incubated with sections of adult pig retina (bright field; **A**), anti-Rs1 antibody (**B**) demonstrated strong immunoreactivity within the interphotoreceptor matrix surrounding photoreceptor inner (IS) and outer segments (OS), as well as outlining cell bodies in the scleral region of the outer nuclear layer (ONL, arrow). There was equally prominent staining in the outer plexiform layer (OPL) and a subset of cells within the inner nuclear layer (INL), with staining percolating down through the inner plexiform layer (IPL) and visible in patches at the level of the ganglion cell (GCL) and nerve fiber (NFL) layers. Scale bar in **B** represents 30 μm. **C**: Western blots of retinal protein extracts prepared from adult pig retinas and run under non-reducing conditions (-β) demonstrated a prominent immunoreactive band about 25 kDa, and a high molecular weight band about 135 kDa. This latter disappeared in reducing conditions (+β) conditions, and represents a multimeric form. Molecular weight (MW) markers (in kDa) are shown to the left of the blots.

from Sigma Life Science Technologies (Cergy Pontoise, France).

Elution of retinoschisin and interacting proteins: Eyes (about 25) from freshly killed adult domestic pigs were enucleated and transported from the slaughterhouse to the laboratory on crushed ice, where the retinas were dissected out as described previously [28]. They were then washed three times in 50 ml of cold 0.1 M phosphate buffered saline (PBS), pH 7.4, containing protease inhibitors (N-ethyl maleimide, 625 mg/l; phenylmethylsulfonyl fluoride, 150 mg/l). They were ground in a 50 ml that contained Tris HCl (50 mM, NaCl 0.5 M, Urea 2 M, EDTA 50 mM, pH 7.4, plus protease inhibitors using the same concentration as noted). The volume was adjusted to 100 ml and stirred overnight at 4 °C on a magnetic stirrer, after which the supernatant was collected and dialyzed against PBS (3 changes, 1 l each) at 4 °C. The extract was centrifuged at 45,000x g for 1 h, and Rs1 was purified by clearing the extract on gelatin-Sepharose, then passed over either a monoclonal (D5) antilaminin IgG/Sepharose affinity column or a polyclonal anti-Rs1 IgG/Sepharose column. Anti-Rs1 and antilaminin β2 antibody affinity columns were prepared by cyanogen bromide activation of Sepharose beads (1 g) previously published methods [29], and packed in mini-columns (length 5 cm, diameter 0.5 cm). Columns were connected to an automated fraction collector, with UV monitoring of 100 µl fractions at OD_{280}. The columns were washed repeatedly with PBS until the eluate returned to baseline values, and proteins eluted with 1 M acetic acid. In control experiments, protein extracts were loaded onto BSA-Sepharose columns and eluted in the same way.

Preparation of retinal layers: Different isolated strata of retina were prepared from 35-day-old C57 mice by planar vibratome sectioning as described before [30]. Briefly, neural retinas were dissected carefully to avoid mechanical disruption of layers, then cemented onto a gelatin block, photoreceptor face down. The vibratome blade was progressively lowered until just in contact with the inner limiting membrane, then successive cuts of 40 µm to remove the ganglion cell layer (GCL), and part of the inner plexiform layer (IPL), 60 µm to remove the inner nuclear layer (INL) and 120 µm to remove the outer nuclear layer (ONL) were performed. Light microscope monitoring of fractions was used to control purity of each fraction, based on morphological criteria (presence of abundant blood vessels and nerve fiber tracts in GCL; heterogeneous cell body sizes and blood vessels in INL; and regular cell body packing and outer segments in ONL). In addition, RT-PCR analysis of transcripts specific to INL (mGluR6, specific to rod bipolar cells [31]) and rhodopsin (specific to rods [32]; Table 1) were used to verify purity. Samples were collected in clean eppendorf tubes and immediately frozen in liq-

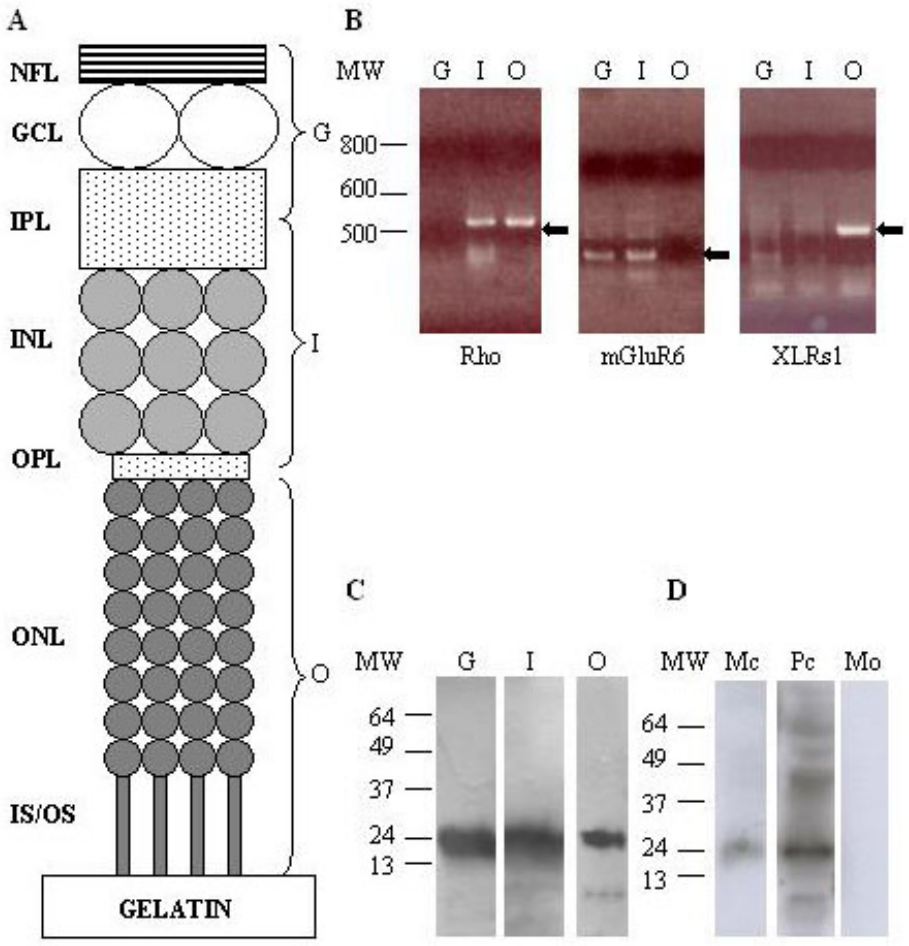

Figure 2. Vibratome separation of retinal layers and RT-PCR and western blot analyses of Rs1. **A**: In schematic representation, adult mouse retinas were placed photoreceptor-side down on a gelatin block and sectioned at three levels to separate ganglion cell layer (G), inner nuclear layer (I) and outer nuclear layer (O). **B**: These samples were analyzed by RT-PCR for the presence of specific markers and Rs1 mRNA. Amplification of rhodopsin-specific primers (Rho) detected transcripts in O as expected, but also in I, indicating contamination of the latter with photoreceptor material. There were no rhodopsin transcripts in G. Amplification of mGluR6-specific primers revealed product in I as expected, and also in G from inner plexiform layer (IPL). There was no signal in O. Rs1 transcripts were only detectable in O. **C**: Anti-Rs1 western blotting of the three samples showed dense bands about 25 kDa in each fraction. **D**: Anti-Rs1 western blotting of conditioned medium from adult pig photoreceptor cultures (Mc) also revealed an immunopositive band of about 25 kDa, also seen in photoreceptor cell extracts (Pc) but not in medium alone (Mo). Molecular weight (MW) markers are shown to the left of each panel in base pairs for **B** and in kDa for **C**,**D**.

uid nitrogen until use in western blotting and RT-PCR analyses.

Preparation of photoreceptor cultures: Highly enriched cultures of rod and cone photoreceptors were prepared from postmortem adult pig retinas using methods described previously [28]. Briefly, following dissection and digestion in papain, cells from the first two supernatants were collected and seeded at an initial density of $5x10^6$ in 35 mm tissue culture dishes in Neurobasal A medium supplemented with 2% fetal calf serum. After 2 days in vitro, medium was replaced with chemically defined medium, Neurobasal A containing B27 supplement. After a further 2 days in vitro, medium was replenished and left for a further 24 h. Medium (1 ml) was then collected and centrifuged at 10,000x g for 10 min, and soluble proteins were precipitated by TCA treatment, resuspended in 50 µl Laemmli buffer and analyzed by western blotting (see the fourth paragraph below).

Immunofluorescence analyses: Pig retinas were obtained from eyes collected at the slaughter house. Tissues were fixed in 4% paraformaldehyde in PBS for 2-6 h, then embedded in Tissue Tek (Sakura Finetek Europe BV, Zoeherwoude, Netherlands), frozen and sectioned by cryostat. The sections were blocked in PBS containing 0.1% bovine serum albumin (BSA), 0.1% Tween 20, 10% normal goat serum and 0.1% sodium azide (buffer A), then incubated overnight at 4 °C in the different primary antibodies (as indicated in the text and figure legends) or lectin diluted in the same buffer. Secondary antibody incubation was performed at room temperature for 60 min with Alexa (594 or 488) goat anti-rabbit or anti-mouse IgG conjugated antibodies (Molecular Probes Ltd., Eugene, OR). Sections were then washed thoroughly and mounted in PBS: glycerol for observation using either a Nikon Optiphot-2 fluorescence microscope equipped with differential interference contrast objectives, or by a confocal laser scanning microscope (Zeiss LSM 510 v2.5) scanning device mounted on a Zeiss Axiovert 100 inverted microscope.

Protein sequencing: Protein sequencing was performed with minor modifications of published methods [33]. Briefly, the eluate from the Rs1 column was resolved on a polyacrylamide gel in presence of 2-mercaptoethanol. The band of interest was excised and digested with trypsin. Analysis of the digest was performed at the Protein Sequencing Laboratory, IGBMC Strasbourg, with matrix-assisted laser desorption time-of-flight mass spectrometry performed on a Finnigan Lasermat 200 [34].

Reverse transcriptase polymerase chain reaction: RNA was purified from sheets obtained by vibratome sectioning of two adult normal (C57) mice retinas using the RNAeasy kit (Qiagen SA, Courtaboeuf France). RNA concentrations from pooled GCL, INL, and ONL fractions varied from 8.6-12.6 ng/µl. PCR amplifications using the different primer pairs listed in Table 1 were performed as follows: denaturation 2 min at 94 °C, 35 cycles at 94 °C for 30 s, 55 °C for 30 s and 72 °C for 1 min, with a final extension period at 72 °C of 7 min. In addition, mRNA loading was checked with PCR primers for the housekeeping enzyme glycerol-6-phosphate dehydrogenase (data not shown). The experiments were repeated three times with identical results.

Western blotting: Total protein levels of single retinal layers were determined by Bradford assay, using an initial series of retinal preparations, as approximately 350-400 µg for ONL, 150-200 µg for INL, and 25-50 µg for GCL. Retinal layers were resuspended in 35 µl of Laemmli buffer, then run on 10% SDS-PAGE [35], the total contents of each separate fraction run on a single lane. Prestained low molecular weight range markers were run on a parallel lane. Proteins were transferred onto nitrocellulose membranes using a standard gel transfer apparatus, Tris 25 mM, glycine 0.192 M, methanol 20% for 1 h at 100 V [36]. The membrane was re-equilibrated in PBS-Tween 0.5% and incubated in PBS-5% fat-free milk for 1 h. After rinsing in PBS-Tween, the membrane was incubated in primary antibody overnight, rinsed three times in PBS-Tween and incubated in secondary antibody for 2 h, then rinsed three times in PBS-Tween. Immunoreactive bands were visualized using a Pierce Super Signal Substrate Kit (Pierce Biotechnology Inc., Rockford, IL) according to the manufacturer's instructions. BioMax films were placed in contact with membranes for less than 25 s and developed according to the manufacturer's instructions.

RESULTS

Distribution of retinoschisin: As previously published [22] for retinas from other mammalian species, immunostaining

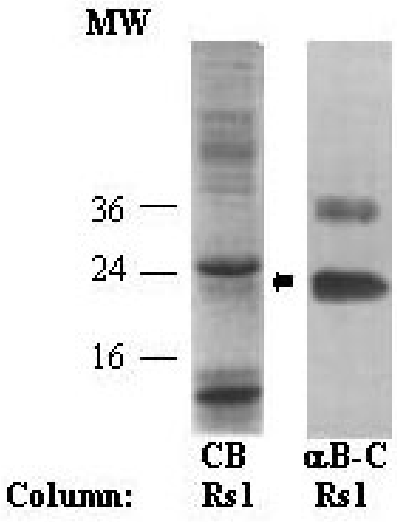

Figure 3. Interaction of retinoschisin with αB-crystallin. Left lane: Low molecular mass proteins eluted from Rs1 column and αB crystallin western blotting. Coomassie blue stained low molecular mass (<60 kDa) fraction showed multiple bands between 50 and 60 kDa, and major bands at about 25 and 10 kDa. The 25 kDa band represents Rs1 itself. Excision and sequencing of the band located just below (indicated by an arrow) identified this 24 kDa species as αB crystallin. Right lane: Western blotting of same eluate using anti-αB crystallin antibody indicated strong immunoreactivity of 23 kDa band, and moderate staining of about 38 kDa band, possibly a dimer. Molecular weight (MW) standards in kDa shown on left.

of adult pig retinal sections with anti-Rs1 antiserum showed intense labeling at the level of the interplexiform matrix (IPM) surrounding the photoreceptor inner segments. Additional label was seen surrounding some photoreceptor cell bodies and their processes within the ONL, principally lying along the scleral margin as well as within the outer plexiform layer (OPL) and in a subpopulation of INL neurones extending down their axons into the IPL (Figure 1). Immunohistochemical labeling was also detectable within the GCL and nerve fiber layer (NFL), although less intensely compared to other layers. Preadsorption of the Rs1 antibody with 100x excess immunizing peptide completely blocked all staining (data not shown).

These immunohistochemical data were complemented by western blotting and RT-PCR studies of retinal distributions of Rs1 protein and *xlrs1* mRNA, respectively. Using a vibratome technique we separated adult mouse retina into three fractions; ONL (containing exclusively photoreceptor cell bodies and distal portions of Müller glia), INL (containing a mixture of bipolar, amacrine and Muller glial cell bodies), and GCL (containing retinal ganglion cells and their axons, as well as displaced amacrine cells and astrocytes). The protocol is shown schematically in Figure 2A. RT-PCR analyses were performed on mRNA prepared from single isolated samples. Quality and purity of the respective RNA preparations was confirmed by amplification of the cell-specific markers mGluR6 (bipolar cells) and rhodopsin (rods). Rhodopsin transcripts were detected in the ONL and INL (indicating con-

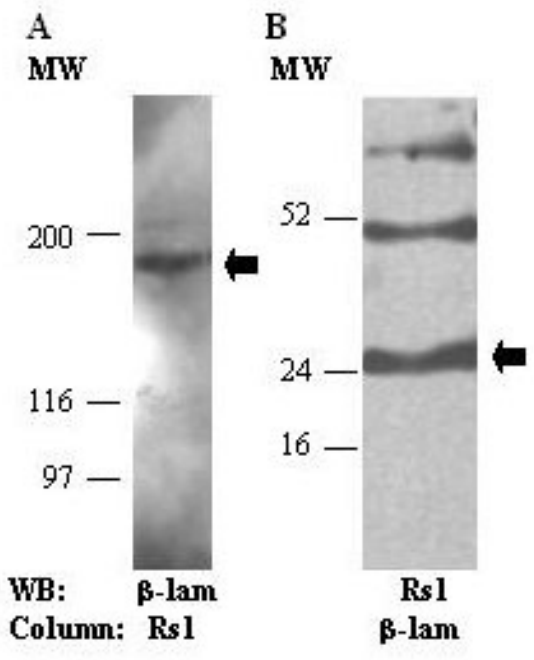

Figure 5. Rs1 and β2 laminin show potential interactions. **A**: Western blotting of eluate derived from anti-Rs1 affinity columns contained a β2 laminin-immunopositive band at about 180 kDa. **B**: Western blotting of eluate derived from anti-β2 laminin affinity columns contained Rs1-immunoreactive bands at about 25, 50, and 75 kDa. Molecular weight (MW) is given to the left of each blot.

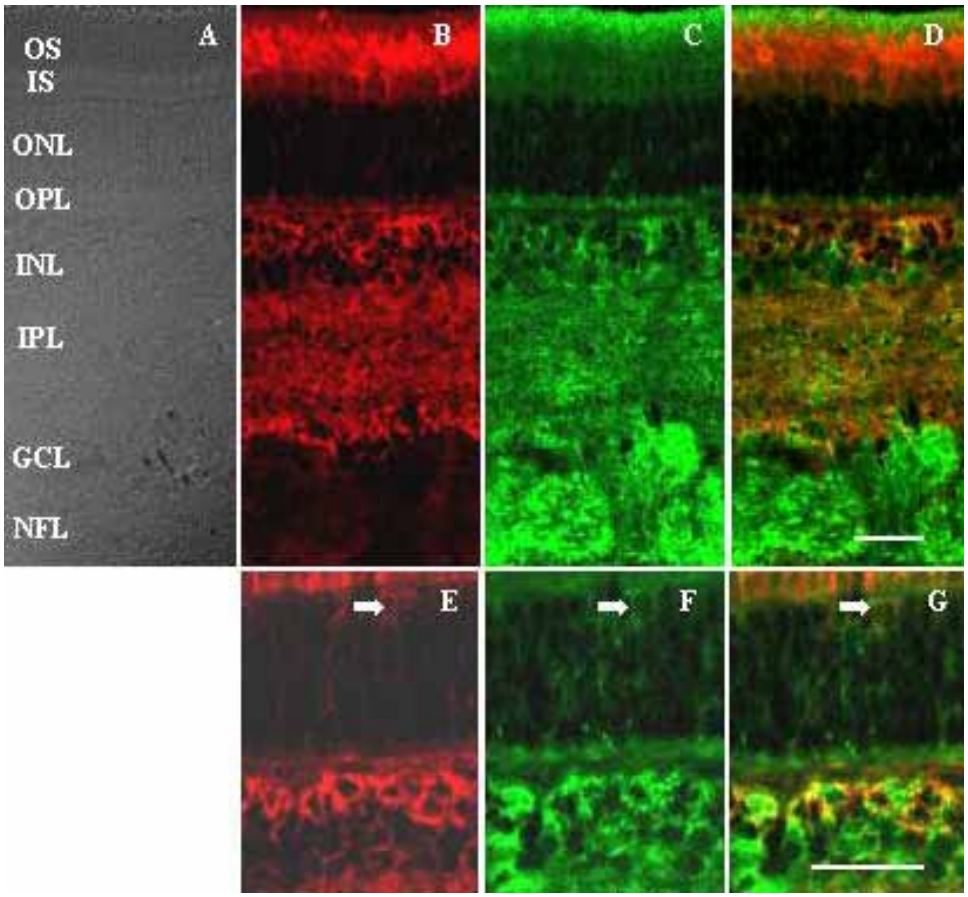

Figure 4. Double label immunohistochemistry of Rs1 and αB crystallin in adult pig retina. Frozen sections of retina (**A**) were co-incubated with antibodies to Rs1 (**B**,**E**) and αB crystallin (**C**,**F**). Staining for both antibodies was strong in the interphotoreceptor matrix and IS and OS, as well as in the INL and IPL. In addition αB crystallin immunoreactivity was intense overlying the nerve fiber fundles in the NFL. Staining for both proteins was moderate within the ONL, outlining cell bodies (**E**,**F**). Overlay of the two images (**D**,**G**) showed label co-segregated within the proximal interphotoreceptor matrix, throughout the INL and IPL, and around cells in the ONL (arrows, **E**-**G**). Scale bar in **D** represents 30 μm for Panels **A**-**D**, scale bar in **G** represents 30 μm for Panels **E**-**G**. The inner segments (IS), outer segments (OS), outer nuclear layer (ONL), the outer plexiform layer (OPL), inner nuclear layer (INL), inner plexiform layer (IPL), ganglion cell layer (GCL), and nerve fiber layer (NFL) are identified.

tamination of the latter by rod mRNA), but not in the GCL. mGluR6 product was observed in the GCL and INL, but not in the ONL (Figure 2B). *xlrs1* transcripts were only found in the ONL with a clear band observed at the expected product size (507 bp, Figure 2B). *xlrs1* product transcripts were undetectable in the INL and GCL samples under the conditions used (Figure 2B). With respect to the western blotting analyses from similar fractions obtained from parallel samples, we observed an immunoreactive band of about 25 kDa in all three samples (Figure 2C). Finally, Rs1 protein was also detected in media conditioned by rod and cone photoreceptors during 24 h. It was also present in cell extracts prepared from the same cells, but was not found in medium that had not been incubated in the presence of cells (Figure 2D).

Interaction of retinoschisin with αB-crystallin: A crude total protein extract prepared from 25 pig retina was loaded onto the anti-Rs1 column, and after extensive washing with PBS the column was eluted with 1 M acetic acid. The eluate was resolved on SDS-Page and stained with Coomassie Blue. Many proteins eluted at molecular masses >60 kDa, but relatively few were visible at lower weights (Figure 3, left lane). The band at about 25 kDa represented Rs1 itself (as demonstrated by immunoblotting: data not shown). We chose to excise the band immediately below Rs1 (i.e., band at about 23 kDa) and process it for mass spectrometric sequence analysis after digestion with trypsin. Three peptides derived from this digestion were identified as corresponding to αB-crystallin, with an identical match to 28% of the protein. To confirm this result, we performed a western blot of the eluate using anti αB-crystallin antibody. In the right lane of Figure 3, a prominent band of about 23 kDa is present, in addition to another band at about 40 kDa which might be a dimer of αB-crystallin.

Double immunostaining of adult porcine retinal sections with monoclonal anti-αB-crystallin and polyclonal anti-Rs1 revealed partially overlapping distributions. αB-crystallin immunoreactivity was observed mainly within the outer IPM, although staining was also seen in the proximal IPM at the same level as Rs1. In addition, the two immunolabels were observed surrounding photoreceptor cell bodies in the ONL,

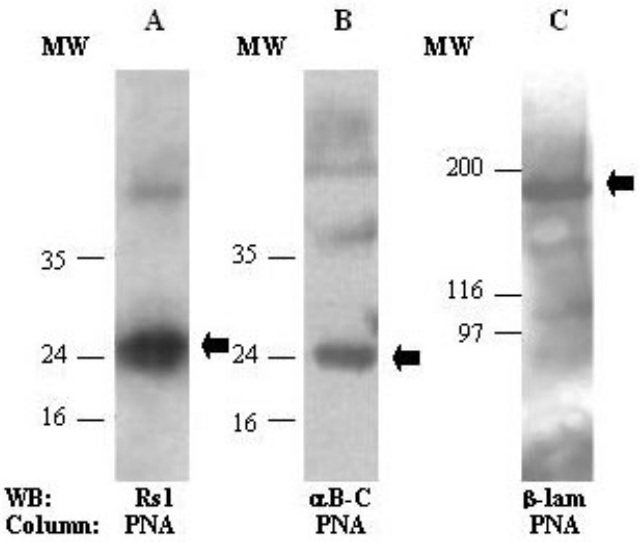

Figure 7. Peanut agglutinin affinity columns retain Rs1, αB crystallin and β2 laminin. When pig retinal extracts are eluted from PNA columns using the sugar competitor, western blotting for Rs1 (**A**), αB crystallin (αB-C; **B**) and β2 laminin (β-lam; **C**) all give immunoreactive bands of appropriate masses at 25, 23, and 180 kDa (arrows). Molecular weights (MW) are given in kDa to the left of each blot.

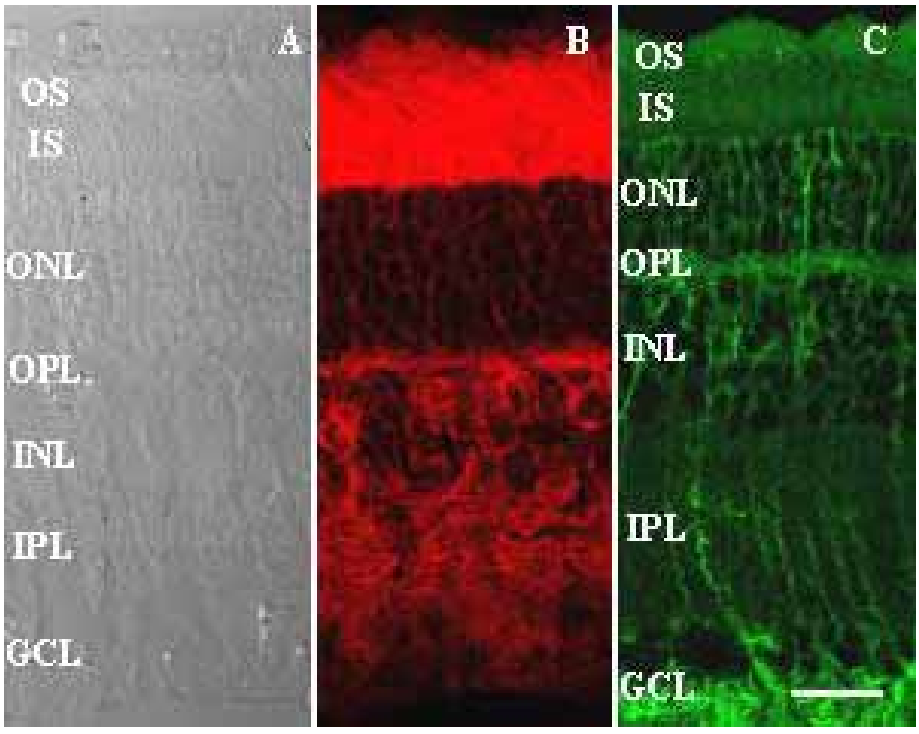

Figure 6. Immunohistochemistry of Rs1 and β2 laminin shows partial overlap. As before, incubation of adult pig retinal sections (**A**) with Rs1 antibody (**B**) gave strong staining within the interphotoreceptor matrix, OPL, INL, and IPL, as well as outlining cell bodies in the ONL. We were unable to perform double label immunohistochemistry with the D5 anti-β2 laminin antibody, which works exclusively on unfixed tissue, but the distribution pattern for this antibody partly overlapped with that of Rs1, with label surrounding cell bodies in the ONL and INL, binding to the OPL, and following the trajectories of radial Müller glia and their endfeet (**C**). Scale bar in **C** represents 30 μm for all panels. The inner segments (IS), outer segments (OS), outer nuclear layer (ONL), the outer plexiform layer (OPL), inner nuclear layer (INL), inner plexiform layer (IPL), ganglion cell layer (GCL), and nerve fiber layer (NFL) are identified.

and across the INL and IPL (Figure 4). αB-crystallin immunoreactivity was also strong in axon bundles within the NFL. Taken together with the affinity column data, these results suggest that Rs1 interacts with αB-crystallin.

Interaction of retinoschisin with laminin: The Rs1 antibody column retentate was also screened for the presence of β2 laminin by western blotting with a specific antibody. Western blot experiments showed the presence of a high molecular mass band about 180 kDa, corresponding to the β2 chain of laminin 14 and 15 (Figure 5A). To confirm a possible interaction between this extracellular matrix protein and Rs1, retinal protein extract was loaded onto an anti-β2 laminin antibody column and eluted as aforedescribed. Western blotting studies of the eluate with the Rs1 antibody clearly showed the presence of this protein (Figure 5B).

We also performed immunohistochemistry for β2 laminin and Rs1. Although we were unable to perform double labeling, as the D5 monoclonal only works on unfixed tissue, we again observed partially overlapping distribution patterns, though distinct from that seen for aB crystallin. β2 laminin immunostaining was observed within the IPM, surrounding cell bodies in the ONL and INL and outlining Müller cell extensions (Figure 6). Therefore, we conclude that Rs1 also has the potential to interact with laminins 14 and 15.

Interaction of retinoschisin and PNA-binding proteins: In a separate series of experiments, retinal extracts were loaded onto a PNA lectin affinity column and eluted with excess competing sugar (1 M D-galactose). The eluate was probed with antibodies against the three proteins: Rs1, αB-crystallin, and β2 laminin. All three proteins were detected at their approximate expected molecular masses under denaturing conditions (Figure 7). Labeling of adult pig retinal sections with Rs1 and PNA revealed overlapping patterns at the level of the cone matrix sheaths within the IPM, as well as surrounding cell bodies within the ONL (Figure 8). Although there was general correspondence between the two labels within the OPL, PNA was more concentrated on presynaptic terminals while Rs1 localized to postsynaptic structures (Figure 8E-G). Distributions of PNA lectin histochemical staining, αB-crystallin and β-laminin immunoreactivity also shared common domains, all three surrounding cell bodies in the ONL (compare Figure 4C, Figure 6C, and Figure 8C).

DISCUSSION

These studies were aimed at extending the knowledge of Rs1 protein distribution in the retina, and beginning to identify proteins capable of interacting with it and participating in the formation of multimolecular scaffolds that provide the structural basis for the role of Rs1 in stabilizing synaptic organization. The principal findings were as follows western blotting suggests a wider tissue distribution than seen by immunohistochemistry; *xlrs1* mRNA could only be detected in photoreceptor samples; and least two proteins can be implicated in Rs1 binding interactions.

There are major differences in *xlrs1* mRNA and Rs1 protein distribution patterns reported by different laboratories. The original studies coming from the laboratory of Farber demonstrated that *xlrs1* mRNA could only be detected in photoreceptors, highly concentrated at the level of the inner segments [18,19]. Subsequent studies by the same group showed that Rs1 protein was more widespread, and that this was accomplished by directed transport involving the radial Müller glial cells [20,21]. In contrast, we observed that *xlrs1* mRNA persisted in mutant mice lacking rods and cones, and Rs1 protein could be seen on bipolar cells in vitro [22]. Furthermore, the laboratory of Sieving, using more sophisticated staining tech-

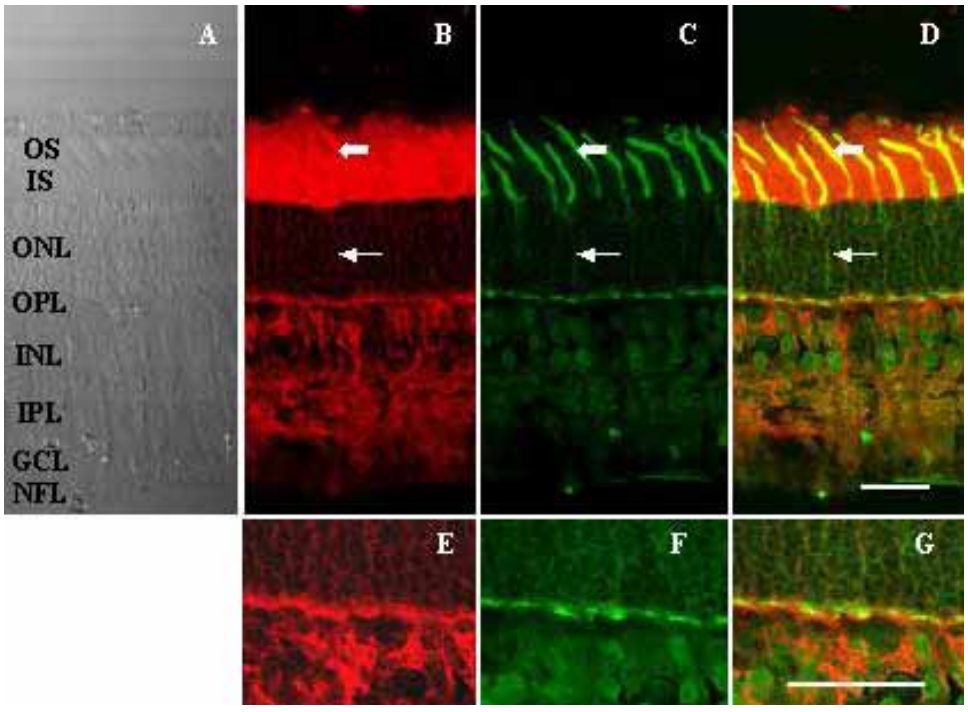

Figure 8. Double staining for Rs1 and PNA gives partial overlap. Adult pig retinal sections (**A**) stained for Rs1 (**B**) or PNA lectin (**C**) showed correspondence of label especially at the level of the cone matrix sheaths (thick arrows), as well as surrounding cell bodies within the ONL (thin arrows). Although the two stains were prominent in the OPL and INL, they did not precisely correspond, with Rs1 localizing more to post-synaptic elements while PNA bound to presynaptic sites (E-G). Scale bar in **D** represents 30 μm for Panels **A**-**D**, and scale bar in **G** represents 30 μm for Panels **E**-**G**. The inner segments (IS), outer segments (OS), outer nuclear layer (ONL), the outer plexiform layer (OPL), inner nuclear layer (INL), inner plexiform layer (IPL), ganglion cell layer (GCL), and nerve fiber layer (NFL) are identified.

niques, was able to detect both mRNA and protein outside the photoreceptors, at the level of the ganglion cells and inner retina [23]. Using a vibratome-based technique developed in our laboratory in order to isolate photoreceptor layers for transplantation [37] or tissue culture [30], we prepared mRNA from fractions of GCL, INL, and ONL. Relative purity of each fraction was assessed by RT-PCR analysis of specific cell markers contained within distinct layers. Hence mGluR6 is expressed uniquely by rod bipolar cells and constitutes a biomarker for INL [31]. Product for this gene was present in INL fractions but not in ONL, showing that the latter were not contaminated by INL cells. However, mGluR6 was also amplified in GCL fractions, which presumably arose from mRNA within cells or processes in the IPL. Similarly, as expected rhodopsin primers were unable to detect message within the GCL, but did show transcripts in the ONL and INL. This latter shows that some cellular material from the ONL was included in the INL preparations. Nevertheless, RT-PCR studies using *xlrs1* primers only revealed mRNA within the ONL, not in the INL or GCL, in accordance with the original findings of Reid and co-workers [18-20]. It is possible we did not detect low levels of expression that would require further rounds of amplification.

Immunohistochemical analyses by different laboratories using different antisera have revealed Rs1 staining to be concentrated within the IPM, ONL, INL, and GCL [18,20,22,23]. Using a newly generated polyclonal antibody (but directed against the same epitope used previously [22]), we also observed abundant labeling of IPM and INL. However western blotting of separated retinal layers using the same antibody exhibited intense staining of GCL fractions. Although part of this staining is accounted for by inclusion of IPL membranes in the GCL fraction, considering the total protein concentrations of GCL preparations were far lower than those used for the other layers, the data indicate a pool of Rs1 residing at this level which is not readily recognized in sections. It is possible that this pool differs in its conformation, partly masking the epitope recognised by the amino terminal antibody, but which is revealed under denaturing gel electrophoresis conditions. Recent studies using highly sensitive immunodetection techniques demonstrated that Rs1 is expressed at the level of the GCL, appearing early in development [23]. This wider distribution is consistent with the inner retinal splitting observed in affected patients and transgenic mice [4,6,24]. We also examined the presence of Rs1 in conditioned medium prepared from highly enriched cultures of adult photoreceptors [28]. Western blotting revealed the presence of a faint band at about 25 kDa after 24 h in culture, indicating that the protein was effectively secreted into the medium. Much higher levels of Rs1 protein were observed in cell lysates prepared from the same cultures, representing either intracellular pools or protein bound to cell surfaces.

Given the secretory nature of Rs1, and the observed effects on synaptic disorganization within the plexiform layers, we reasoned that the protein likely interacts with both other extracellular proteins and transmembrane and intracellular proteins to constitute a complex scaffold involved in stabilizing cellular structure. Importantly, the discoidin domain has been shown to interact with collagen [38]. Also, such multimolecular complexes have been observed in several cases, notably in the interactions of the dystrophin and dystrophin-associated family members with membrane-bound neurotransmitter receptors and the cytoskeleton [39-41], including within the retina [42]. In addition, both dystrophin animal mutants and afflicted humans exhibit features associated with loss of the ERG b wave, as seen in *xlrs1* mutants [43,44]. As techniques such as yeast double hybrid trapping are not particularly suitable for membrane proteins, we chose two complementary approaches to begin searching for candidate Rs1-interacting proteins: screening against potentially relevant ECM proteins, and affinity isolation of binding proteins. Laminins 14 and 15, of chain composition $\alpha4\beta2\gamma3$ and $\alpha5\beta2\gamma3$, are known to be present in the IPM [45], and knockout mice exhibit a retinal phenotype with some resemblances to *xlrs1* -/- mice (ERG b-wave abnormalities), and it was therefore logical to investigate if these laminins could bind to Rs1. Three lines of evidence suggest this may be the case: (1) Rs1 is detected in retentates on laminin antibody columns; (2) laminin is detected in retentates of Rs1 antibody columns; and (3) the two proteins exhibit partial overlap in their retinal distributions.

As revealed by Coumassie blue staining, acid elution of proteins retained on an affinity column prepared using anti-Rs1 antibody produced a wide range of molecular mass species. Sequencing of a selected band running just underneath that of Rs1 itself identified aB crystallin as a binding protein. Several previous reports have shown this member of the crystallin family to be present in the neural retina, notably within photoreceptors and Müller glia [46,47]. It associates tightly with post-Golgi transport vesicles in the photoreceptor cytoplasm [48], has been shown to possess chaperone-like activities [49,50], and is involved in prevention of apoptosis [51]. It is seen to be upregulated in retina subjected to various insults such as light-induced stress or inherited degeneration [52,53]. Thus its association with Rs1 seems plausible, enabling it to be involved in transport and release of Rs1-containing vesicles within the photoreceptor cytosol.

In addition to this investigation, previous studies on Rs1 expression have observed large amounts of protein at the level of the photoreceptor inner segments if not within the subretinal space [19-24]. This localization does not correspond with any apparent function, since Rs1 mutations do not appear to display major defects in photoreceptors themselves [1-7]. Nevertheless, given the prominence of Rs1 immunostaining within this compartment, especially at the level of the cone matrix sheath, it also seemed reasonable to speculate that it may interact with galactose-containing glycoproteins enriched in this space [54]. PNA staining is also seen within the OPL, another site where Rs1 is abundant, although close observation of their binding indicates they do not coincide. It is of interest that not only Rs1 itself, but also $\beta2$ laminin and αB crystallin were present in PNA column retentates. However, it is important to point out that laminins are glycoproteins containing several consensus glycosylation motifs [55], and that galactose itself has been reported to constitute part of the carbohydrate moi-

ety [56]. Furthermore, a large body of data demonstrates that crystallins accept sugar residues through nonenzymatic reactions, termed glycation [50], which occur as a consequence of disease or aging. Thus these proteins could also be pulled down directly by PNA binding, and may not interact through Rs1 or PNA binding proteins.

In conclusion, these studies indicate that Rs1 forms multimolecular complexes with a minimum of two candidate partners, β2 laminin and αB crystallin, and possibly with unidentified glycoconjugates. Although these findings represent only a first step, they provide original data on the molecular components to which Rs1 may bind. Interactions with αB crystallin are most likely to be intracellular, while the association with β2 laminin probably occurs at the level of the extracellular scaffold involved in stabilizing synapses. Use of interphotoreceptor matrix preparations [57] or photoreceptor extracts instead of total proteins, should refine protein-protein interactions. It will be of especial interest to delimit the binding domains involved in these interactions, and to examine whether known mutations in Rs1 affect its ability to bind. For example, since some mutations compromise Rs1 transport and secretion [15,17], αB crystallin association may be diminished.

ACKNOWLEDGEMENTS

MFSC was supported by a grant from the Fondation de France; other sources of financial support included a core grant from INSERM.

REFERENCES

1. Condon GP, Brownstein S, Wang NS, Kearns JA, Ewing CC. Congenital hereditary (juvenile X-linked) retinoschisis. Histopathologic and ultrastructural findings in three eyes. Arch Ophthalmol 1986; 104:576-83.
2. Kellner U, Brummer S, Foerster MH, Wessing A. X-linked congenital retinoschisis. Graefes Arch Clin Exp Ophthalmol 1990; 228:432-7.
3. George ND, Yates JR, Moore AT. Clinical features in affected males with X-linked retinoschisis. Arch Ophthalmol 1996; 114:274-80.
4. Tantri A, Vrabec TR, Cu-Unjieng A, Frost A, Annesley WH Jr, Donoso LA. X-linked retinoschisis: a clinical and molecular genetic review. Surv Ophthalmol 2004; 49:214-30.
5. Peachey NS, Fishman GA, Derlacki DJ, Brigell MG. Psychophysical and electroretinographic findings in X-linked juvenile retinoschisis. Arch Ophthalmol 1987; 105:513-6.
6. Sieving PA, Bingham EL, Kemp J, Richards J, Hiriyanna K. Juvenile X-linked retinoschisis from XLRS1 Arg213Trp mutation with preservation of the electroretinogram scotopic b-wave. Am J Ophthalmol 1999; 128:179-84.
7. Khan NW, Jamison JA, Kemp JA, Sieving PA. Analysis of photoreceptor function and inner retinal activity in juvenile X-linked retinoschisis. Vision Res 2001; 41:3931-42.
8. Sauer CG, Gehrig A, Warneke-Wittstock R, Marquardt A, Ewing CC, Gibson A, Lorenz B, Jurklies B, Weber BH. Positional cloning of the gene associated with X-linked juvenile retinoschisis. Nat Genet 1997; 17:164-70.
9. Springer WR, Cooper DN, Barondes SH. Discoidin I is implicated in cell-substratum attachment and ordered cell migration of Dictyostelium discoideum and resembles fibronectin. Cell 1984; 39:557-64.
10. Baumgartner S, Hofmann K, Chiquet-Ehrismann R, Bucher P. The discoidin domain family revisited: new members from prokaryotes and a homology-based fold prediction. Protein Sci 1998; 7:1626-31.
11. Vogel W. Discoidin domain receptors: structural relations and functional implications. FASEB J 1999; 13:S77-82.
12. Wu WW, Wong JP, Kast J, Molday RS. RS1, a discoidin domain-containing retinal cell adhesion protein associated with X-linked retinoschisis, exists as a novel disulfide-linked octamer. J Biol Chem 2005; 280:10721-30.
13. Shastry BS, Hejtmancik FJ, Trese MT. Recurrent missense (R197C) and nonsense (Y89X) mutations in the XLRS1 gene in families with X-linked retinoschisis. Biochem Biophys Res Commun 1999; 256:317-9.
14. Inoue Y, Yamamoto S, Okada M, Tsujikawa M, Inoue T, Okada AA, Kusaka S, Saito Y, Wakabayashi K, Miyake Y, Fujikado T, Tano Y. X-linked retinoschisis with point mutations in the XLRS1 gene. Arch Ophthalmol 2000; 118:93-6.
15. Wang T, Waters CT, Rothman AM, Jakins TJ, Romisch K, Trump D. Intracellular retention of mutant retinoschisin is the pathological mechanism underlying X-linked retinoschisis. Hum Mol Genet 2002; 11:3097-105.
16. Wu WW, Molday RS. Defective discoidin domain structure, subunit assembly, and endoplasmic reticulum processing of retinoschisin are primary mechanisms responsible for X-linked retinoschisis. J Biol Chem 2003; 278:28139-46.
17. Wang T, Zhou A, Waters CT, O'Connor E, Read RJ, Trump D. Molecular pathology of X linked retinoschisis: mutations interfere with retinoschisin secretion and oligomerisation. Br J Ophthalmol 2006; 90:81-6.
18. Reid SN, Akhmedov NB, Piriev NI, Kozak CA, Danciger M, Farber DB. The mouse X-linked juvenile retinoschisis cDNA: expression in photoreceptors. Gene 1999; 227:257-66.
19. Grayson C, Reid SN, Ellis JA, Rutherford A, Sowden JC, Yates JR, Farber DB, Trump D. Retinoschisin, the X-linked retinoschisis protein, is a secreted photoreceptor protein, and is expressed and released by Weri-Rb1 cells. Hum Mol Genet 2000; 9:1873-9.
20. Reid SN, Yamashita C, Farber DB. Retinoschisin, a photoreceptor-secreted protein, and its interaction with bipolar and muller cells. J Neurosci 2003; 23:6030-40.
21. Reid SN, Farber DB. Glial transcytosis of a photoreceptor-secreted signaling protein, retinoschisin. Glia 2005; 49:397-406.
22. Molday LL, Hicks D, Sauer CG, Weber BH, Molday RS. Expression of X-linked retinoschisis protein RS1 in photoreceptor and bipolar cells. Invest Ophthalmol Vis Sci 2001; 42:816-25.
23. Takada Y, Fariss RN, Tanikawa A, Zeng Y, Carper D, Bush R, Sieving PA. A retinal neuronal developmental wave of retinoschisin expression begins in ganglion cells during layer formation. Invest Ophthalmol Vis Sci 2004; 45:3302-12.
24. Weber BH, Schrewe H, Molday LL, Gehrig A, White KL, Seeliger MW, Jaissle GB, Friedburg C, Tamm E, Molday RS. Inactivation of the murine X-linked juvenile retinoschisis gene, Rs1h, suggests a role of retinoschisin in retinal cell layer organization and synaptic structure. Proc Natl Acad Sci U S A 2002; 99:6222-7.
25. Zeng Y, Takada Y, Kjellstrom S, Hiriyanna K, Tanikawa A, Wawrousek E, Smaoui N, Caruso R, Bush RA, Sieving PA. RS-1 Gene Delivery to an Adult Rs1h Knockout Mouse Model Restores ERG b-Wave with Reversal of the Electronegative Wave-

form of X-Linked Retinoschisis. Invest Ophthalmol Vis Sci 2004; 45:3279-85.
26. Min SH, Molday LL, Seeliger MW, Dinculescu A, Timmers AM, Janssen A, Tonagel F, Tanimoto N, Weber BH, Molday RS, Hauswirth WW. Prolonged recovery of retinal structure/function after gene therapy in an Rs1h-deficient mouse model of x-linked juvenile retinoschisis. Mol Ther 2005; 12:644-51.
27. Libby RT, Hunter DD, Brunken WJ. Developmental expression of laminin beta 2 in rat retina. Further support for a role in rod morphogenesis. Invest Ophthalmol Vis Sci 1996; 37:1651-61.
28. Traverso V, Kinkl N, Grimm L, Sahel J, Hicks D. Basic fibroblast and epidermal growth factors stimulate survival in adult porcine photoreceptor cell cultures. Invest Ophthalmol Vis Sci 2003; 44:4550-8.
29. Cuatrecasas P. Protein purification by affinity chromatography. Derivatizations of agarose and polyacrylamide beads. J Biol Chem 1970; 245:3059-65.
30. Fontaine V, Kinkl N, Sahel J, Dreyfus H, Hicks D. Survival of purified rat photoreceptors in vitro is stimulated directly by fibroblast growth factor-2. J Neurosci 1998; 18:9662-72.
31. Nomura A, Shigemoto R, Nakamura Y, Okamoto N, Mizuno N, Nakanishi S. Developmentally regulated postsynaptic localization of a metabotropic glutamate receptor in rat rod bipolar cells. Cell 1994; 77:361-9.
32. Stryer L. Cyclic GMP cascade of vision. Annu Rev Neurosci 1986; 9:87-119.
33. Aebersold RH, Leavitt J, Saavedra RA, Hood LE, Kent SB. Internal amino acid sequence analysis of proteins separated by one- or two-dimensional gel electrophoresis after in situ protease digestion on nitrocellulose. Proc Natl Acad Sci U S A 1987; 84:6970-4.
34. Chait BT, Kent SB. Weighing naked proteins: practical, high-accuracy mass measurement of peptides and proteins. Science 1992; 257:1885-94.
35. Laemmli UK. Cleavage of structural proteins during the assembly of the head of bacteriophage T4. Nature 1970; 227:680-5.
36. Lunstrum GP, Sakai LY, Keene DR, Morris NP, Burgeson RE. Large complex globular domains of type VII procollagen contribute to the structure of anchoring fibrils. J Biol Chem 1986; 261:9042-8.
37. Mohand-Said S, Hicks D, Simonutti M, Tran-Minh D, Deudon-Combe A, Dreyfus H, Silverman MS, Ogilvie JM, Tenkova T, Sahel J. Photoreceptor transplants increase host cone survival in the retinal degeneration (rd) mouse. Ophthalmic Res 1997; 29:290-7.
38. Curat CA, Eck M, Dervillez X, Vogel WF. Mapping of epitopes in discoidin domain receptor 1 critical for collagen binding. J Biol Chem 2001; 276:45952-8.
39. Cavaldesi M, Macchia G, Barca S, Defilippi P, Tarone G, Petrucci TC. Association of the dystroglycan complex isolated from bovine brain synaptosomes with proteins involved in signal transduction. J Neurochem 1999; 72:1648-55.
40. Ervasti JM, Campbell KP. Membrane organization of the dystrophin-glycoprotein complex. Cell 1991; 66:1121-31.
41. Henry MD, Campbell KP. Dystroglycan: an extracellular matrix receptor linked to the cytoskeleton. Curr Opin Cell Biol 1996; 8:625-31.
42. Claudepierre T, Rodius F, Frasson M, Fontaine V, Picaud S, Dreyfus H, Mornet D, Rendon A. Differential distribution of dystrophins in rat retina. Invest Ophthalmol Vis Sci 1999; 40:1520-9.
43. Pillers DA, Bulman DE, Weleber RG, Sigesmund DA, Musarella MA, Powell BR, Murphey WH, Westall C, Panton C, Becker LE, Worton RG, Ray PN. Dystrophin expression in the human retina is required for normal function as defined by electroretinography. Nat Genet 1993; 4:82-6.
44. Kameya S, Araki E, Katsuki M, Mizota A, Adachi E, Nakahara K, Nonaka I, Sakuragi S, Takeda S, Nabeshima Y. Dp260 disrupted mice revealed prolonged implicit time of the b-wave in ERG and loss of accumulation of beta-dystroglycan in the outer plexiform layer of the retina. Hum Mol Genet 1997; 6:2195-203.
45. Libby RT, Champliaud MF, Claudepierre T, Xu Y, Gibbons EP, Koch M, Burgeson RE, Hunter DD, Brunken WJ. Laminin expression in adult and developing retinae: evidence of two novel CNS laminins. J Neurosci 2000; 20:6517-28.
46. Xi J, Farjo R, Yoshida S, Kern TS, Swaroop A, Andley UP. A comprehensive analysis of the expression of crystallins in mouse retina. Mol Vis 2003; 9:410-9.
47. Jones SE, Jomary C, Grist J, Thomas MR, Neal MJ. Expression of alphaB-crystallin in a mouse model of inherited retinal degeneration. Neuroreport 1998; 9:4161-5.
48. Deretic D, Aebersold RH, Morrison HD, Papermaster DS. Alpha A- and alpha B-crystallin in the retina. Association with the post-Golgi compartment of frog retinal photoreceptors. J Biol Chem 1994; 269:16853-61.
49. Horwitz J. Alpha-crystallin can function as a molecular chaperone. Proc Natl Acad Sci U S A 1992; 89:10449-53.
50. Groenen PJ, Merck KB, de Jong WW, Bloemendal H. Structure and modifications of the junior chaperone alpha-crystallin. From lens transparency to molecular pathology. Eur J Biochem 1994; 225:1-19.
51. Mao YW, Liu JP, Xiang H, Li DW. Human alphaA- and alphaB-crystallins bind to Bax and Bcl-X(S) to sequester their translocation during staurosporine-induced apoptosis. Cell Death Differ 2004; 11:512-26.
52. Sakaguchi H, Miyagi M, Darrow RM, Crabb JS, Hollyfield JG, Organisciak DT, Crabb JW. Intense light exposure changes the crystallin content in retina. Exp Eye Res 2003; 76:131-3. Erratum in: Exp Eye Res 2003; 77:121-2.
53. Cavusoglu N, Thierse D, Mohand-Said S, Chalmel F, Poch O, Van-Dorsselaer A, Sahel JA, Leveillard T. Differential proteomic analysis of the mouse retina: the induction of crystallin proteins by retinal degeneration in the rd1 mouse. Mol Cell Proteomics 2003; 2:494-505.
54. Hageman GS, Johnson LV. Biochemical characterization of the major peanut-agglutinin-binding glycoproteins in vertebrate retinae. J Comp Neurol 1986; 249:499-510.
55. Durkin ME, Bartos BB, Liu SH, Phillips SL, Chung AE. Primary structure of the mouse laminin B2 chain and comparison with laminin B1. Biochemistry 1988; 27:5198-204.
56. Arumugham RG, Hsieh TC, Tanzer ML, Laine RA. Structures of the asparagine-linked sugar chains of laminin. Biochim Biophys Acta 1986; 883:112-26.
57. Uehara F, Yasumura D, LaVail MM. New isolation method of retina and interphotoreceptor matrix. Exp Eye Res 1989; 49:305-9.

The print version of this article was created on 10 Aug 2006. This reflects all typographical corrections and errata to the article through that date. Details of any changes may be found in the online version of the article.